

2-2012


Decorin antagonizes the angiogenic network: Concurrent inhibition of met, hypoxia inducible factor 1 α , vascular endothelial growth factor A, and induction of thrombospondin-1 and tiMP3

Thomas Neill
Thomas Jefferson University

Hannah Painter
Thomas Jefferson University

Simone Buraschi
Thomas Jefferson University

Rick T. Owens
Follow this and additional works at: <https://jdc.jefferson.edu/pacbfplife>
LifeCell Corporation, Branchburg, New Jersey

 Part of the [Medical Cell Biology Commons](#), [Medical Pathology Commons](#), and the [Medical](#)

[Pharmacology Commons](#)
Michael P. Lisanti
Thomas Jefferson University

[Let us know how access to this document benefits you](#)

See next page for additional authors
Recommended Citation

Neill, Thomas; Painter, Hannah; Buraschi, Simone; Owens, Rick T.; Lisanti, Michael P.; Schaefer, Liliana; and Iozzo, Renato V., "Decorin antagonizes the angiogenic network: Concurrent inhibition of met, hypoxia inducible factor 1 α , vascular endothelial growth factor A, and induction of thrombospondin-1 and tiMP3" (2012). *Department of Pathology, Anatomy, and Cell Biology Faculty Papers*. Paper 97.
<https://jdc.jefferson.edu/pacbfplife/97>

This Article is brought to you for free and open access by the Jefferson Digital Commons. The Jefferson Digital Commons is a service of Thomas Jefferson University's [Center for Teaching and Learning \(CTL\)](#). The Commons is a showcase for Jefferson books and journals, peer-reviewed scholarly publications, unique historical collections from the University archives, and teaching tools. The Jefferson Digital Commons allows researchers and interested readers anywhere in the world to learn about and keep up to date with Jefferson scholarship. This article has been accepted for inclusion in Department of Pathology, Anatomy, and Cell Biology Faculty Papers by an authorized administrator of the Jefferson Digital Commons. For more information, please contact: JeffersonDigitalCommons@jefferson.edu.

Authors

Thomas Neill, Hannah Painter, Simone Buraschi, Rick T. Owens, Michael P. Lisanti, Liliana Schaefer, and Renato V. Iozzo

DECORIN ANTAGONIZES THE ANGIOGENIC NETWORK: CONCURRENT INHIBITION OF MET, HIF-1A AND VEGFA AND INDUCTION OF THROMBOSPONDIN-1 AND TIMP3*

Thomas Neill[‡], Hannah Painter[‡], Simone Buraschi[‡], Rick T. Owens[§], Michael P. Lisanti[¶], Liliana Schaefer^{||}, and Renato V. Iozzo^{‡1}

From the [‡]Department of Pathology, Anatomy and Cell Biology, and the Cancer Cell Biology and Signaling Program, Kimmel Cancer Center, Thomas Jefferson University, Philadelphia, Pennsylvania 19107, [§]LifeCell Corporation, Branchburg, New Jersey 08876, [¶]Stem Cell Biology and Regenerative Medicine Center, and the Kimmel Cancer Center, Thomas Jefferson University, Philadelphia, Pennsylvania, 19107, and ^{||}Goethe University, Frankfurt, Germany
Running head: Decorin Antagonizes Angiogenesis

¹To whom correspondence should be addressed: Renato V. Iozzo, Department of Pathology, Anatomy and Cell Biology, 1020 Locust Street, Room 249 JAH, Thomas Jefferson University, Philadelphia, PA 19107. Tel.:215-503-2208; Fax: 215-923-7969; E-mail: iozzo@kimmelcancercenter.org

Capsule

Background: Decorin antagonizes multiple receptor tyrosine kinases, such as Met, to suppress tumorigenesis.

Results: Decorin promotes angiostasis by blocking HIF-1 α and β -catenin to inhibit VEGFA and MMP2/9 activity concurrent with thrombospondin-1 and TIMP3 induction.

Conclusion: Decorin abrogates the pro-angiogenic HGF/Met signaling axis, thereby repressing VEGFA-mediated angiogenesis under normoxia.

Significance: Soluble decorin attenuates early tumor growth by preventing normoxic angiogenic signaling through the Met receptor.

Decorin, a small leucine-rich proteoglycan, inhibits tumor growth by antagonizing multiple receptor tyrosine kinases including EGFR and Met. Here, we investigated decorin during normoxic angiogenic signaling. An angiogenic PCR array revealed a profound decorin-evoked transcriptional inhibition of pro-angiogenic genes, such as *HIF1A*. Decorin evoked a reduction of HIF-1 α and VEGFA in MDA-231 breast carcinoma cells expressing constitutively-active HIF-1 α . Suppression of Met with decorin or siRNA evoked a similar reduction of VEGFA by attenuating downstream β -catenin signaling. These data establish a non-canonical role for β -catenin in regulating VEGFA expression. We found that exogenous decorin induced expression of thrombospondin-1 and TIMP3, two powerful angiostatic agents. In contrast, decorin suppressed both the expression and enzymatic activity of MMP9 and MMP2, two pro-angiogenic proteases. Our data establish a novel duality for decorin as a suppressor of tumor angiogenesis under normoxia by simultaneously down-regulating potent pro-angiogenic factors and inducing endogenous anti-angiogenic agents.

A pertinent concept in the field of tumorigenesis is the critical role of the extracellular matrix as an active participant in the regulation of diverse cell processes and signaling events that form an environment signified by ever-changing flux (1). These diverse cellular processes, permissive for tumor progression, are often modulated by matrix constituents that culminate to affect tumor invasion, metastasis and angiogenesis (2).

Various members of the proteoglycan gene family are intimately involved in regulating tumor angiogenesis by directly affecting key downstream signaling pathways via interaction with ligands and their cognate receptors (3-5). Decorin, a prototypical member belonging to a superfamily of 18 individually-encoded gene products collectively known as the small leucine-rich proteoglycans (SLRPs)² (6-8), has been implicated in regulating angiogenesis.

Decorin was originally characterized to bind fibrillar collagen, primarily type I, and to regulate fibrillogenesis (9-16), tissue mechanical properties (17-21), and wound healing and fibrosis (22,23). Decorin also regulates the entry of *Borrelia burgdorferi* spirochetes—the causative agent of Lyme disease—into the dermis (24,25) and several other pathophysiological processes including dentin and bone mineralization (26-28), skeletal muscle homeostasis (29), vertebrate convergent extension (30), bone marrow stromal cell fate (31), myocardial infarction (32), corneal transparency (33), various types of nephropathies (34-38), and tumor inflammation (39).

In the context of cancer, decorin was first identified as a proteoglycan highly induced in the stroma of colon cancer (40,41) suggesting that decorin might counteract the growth of malignant cells in a paracrine fashion. Subsequently, it was discovered that decorin evokes downregulation of multiple receptor tyrosine kinases (RTKs) including the EGFR (42-45) as well as to other ErbB family members (46). This signaling leads to marked tumor growth inhibition (47), induction of the cyclin-dependent kinase inhibitor p21^{WAF1/Cip1} (p21) (48,49) and mobilization of intracellular Ca²⁺ stores in cancer cells (50). Moreover, decorin has been found to

antagonize the Met proto-oncogene (51) by receptor internalization via caveolar-mediated endocytosis (52), resulting in cessation of signaling analogous to EGFR (53). This mode of action is in stark contrast to clathrin-mediated endocytosis of Met (54) which enables Met to maintain a prolonged activation of downstream signaling (55).

Although decorin-null mice are apparently normal (9), double mutant mice lacking decorin and p53 succumb very early to very aggressive lymphomas suggesting that loss of decorin is permissive for tumorigenesis (56). This concept is further corroborated by a recent study using decorin-null mice in a different genetic background. Under these conditions, lack of decorin causes intestinal tumor formation, a process exacerbated by exposing the mice to a high-fat diet (57). Conversely, delivery of decorin gene or protein retards the growth of a variety of cancers (58-65).

The role of decorin in tumor angiogenesis is controversial. Previous reports have delineated a pro-angiogenic response, primarily on normal, non-tumorigenic endothelial cells (66-68) or through loss of decorin in the cornea (69). Interestingly, an anti-angiogenic role for decorin has also been described in various settings (70-72) and as an angiostatic agent targeting tumor cells which exhibit dysregulated angiogenesis via a reduction in vascular endothelial growth factor (VEGF) production (73). The apparent dichotomous effects reported for decorin on endothelial cells and the perceived function on the tumor itself creates a scenario where decorin is able to differentially modulate angiogenesis. This is further substantiated by a recent report where the expression of decorin was evaluated as a function of tumor malignancy. Sarcomas exhibited almost a complete absence of decorin in contrast to hemangiomas, where decorin was predominantly detected in the surrounding stroma (74). Aside from the potent pro-migratory, pro-invasive, and pro-survival roles inherent with aberrant Met activation (75), the Met signaling axis is powerfully pro-angiogenic, specifically promoting VEGFA mediated angiogenesis (76,77). These observations coupled to the discovery of rapid and sustained physical downregulation of Met evoked by nanomolar concentrations of recombinant decorin (51,52) led us to hypothesize that decorin could inhibit angiogenesis via downregulation of the Met signaling axis.

In the present study, we provide mechanistic insight supporting a functional link between decorin and the Met signaling axis vis-à-vis the regulation of pathological VEGF-mediated angiogenesis. The angiostatic effects resulting in a marked inhibition of VEGFA occur at both the transcriptional and post-transcriptional levels with upstream signaling occurring

via Met, which is antagonized by decorin. Further, our findings indicate a novel induction of thrombospondin-1 and TIMP3, coincident with the suppression of pro-angiogenic molecules. Thus, our data reinforce and extend the critical role for decorin as an antagonist of tumor angiogenesis.

EXPERIMENTAL PROCEDURES

Cells and Materials—HeLa squamous carcinoma and MDA-MB-231 triple-negative breast carcinoma cells were obtained from American Type Culture Collection (Manassas, VA). MDA-MB-231 (hereafter referred to as MDA-231 including derivative MDA-231 cell lines), MDA-231(GFP+), wtHIF-1 α and mutHIF-1 α cells were previously described (78). Cells were maintained in Dulbecco's Modified Eagle's Medium supplemented with 10% fetal bovine serum (FBS) (SAFC Biosciences, Lenexa, KS) as well as with 100 μ g/ml of penicillin/streptomycin (MediaTech, Manassas, VA). Human umbilical vein endothelial cells (HUVECs) were purchased from Lifeline cells Technology (Walkersville, MD) and used only within the first 5 passages. Primary antibodies against VEGFA (sc-152), and Met (Met-C12, Sc-10) were from Santa Cruz Biotechnology (Santa Cruz, CA); rabbit polyclonal anti- β -catenin (ab16051) and anti-MMP14 (ab3644) antibodies were purchased from Abcam Inc. (Boston, MA); mouse monoclonal anti- β -actin antibody was from Sigma-Aldrich (St. Louis, MO). The anti-perlecan antibody has been previously characterized (79,80).

Slot Blot Assay for the Analysis of Secreted VEGFA—Cells were treated with decorin protein core in DMEM for 24 h. Conditioned medium was collected, filtered, then briefly centrifuged and applied to the slot blot sample acceptor. Suction was applied for 30 min to ensure attachment to the nitrocellulose membrane, which was washed, and blocked overnight. Incubation with a primary antibody specific for the secreted factor was followed by application of an infrared-labeled secondary antibody and subsequent visualization and quantification via the Odyssey Infrared System.

Transient Knockdown of Met Receptor—Transient knockdown of the Met receptor was achieved via utilization of a cocktail consisting of three validated siRNAs specific for Met mRNA (Met siRNA sc-29397 Santa Cruz). Briefly, six-well plates were seeded with 2×10^5 HeLa cells, followed by incubation overnight at 37°C until cultures were 70% confluent. Targeting siRNA duplex at a final concentration of 80 pM was added to diluted Lipofectamine 2000 (Invitrogen, Grand Island, NY) in OPTI-MEM I Reduced Serum Medium (GIBCO, Carlsbad, CA). Transfection was carried out for 48 h at 37°C and the cells were then treated with DMEM or decorin (500 nM) for an additional 24 h.

Verification of siRNA-mediated knockdown of the Met receptor was determined via immunoblotting using Met specific antibodies.

Quantitative Real Time PCR Analysis—Gene expression analysis by quantitative real-time polymerase chain reaction (qPCR) was carried out as described before (81) with minor modifications. Briefly, sub-confluent ($\sim 1.5 \times 10^6$ cells) 3.5 cm² dishes of HeLa cells were treated for 24 h with either PBS (mock) or 500 nM decorin protein core in DMEM. After incubation, cells were lysed directly in 500 μ l of TRIzol Reagent (Invitrogen). Tumor RNA was obtained as described before (52). Subsequent isolation of RNA and cDNA synthesis proceeded as for cell culture. As such, total RNA (1 μ g) was annealed with Oligo (dT) primers and cDNA was synthesized utilizing the SuperScript Reverse Transcriptase II (Invitrogen) according to the manufacturer's instructions. Gene specific primers were verified before use (supplemental Table 1). The target genes and endogenous housekeeping gene (*ACTB*) amplicons were amplified in independent reactions using the Brilliant SYBR Green Master Mix II (Agilent Technologies, Cedar Creek, TX). All samples were run in quadruplicate on an Mx3005P Real Time PCR platform (Agilent) or on a LightCycle 480-II (Roche, Basel, Switzerland) and the cycle number (Ct) was obtained for each independent reaction. Fold change determinations were made utilizing the Comparative Ct method for gene expression analysis. Briefly, Delta Ct (Δ Ct) values are representative of the normalized gene expression levels with respect to *ACTB* (β -actin as the endogenous housekeeping control). Delta Delta Ct ($\Delta\Delta$ Ct) values represent the experimental cDNA (samples treated with 500 nM decorin protein core) minus the corresponding gene levels of the calibrator sample (samples treated with PBS mock). Finally, the reported fold change represents an average of the fold changes as calculated using the double Δ Ct method ($2^{-\Delta\Delta\text{Ct}}$). Data derive from two-three independent trials for each gene of interest.

RT² Profiler PCR Array—The specific expression of angiogenic genes was evaluated using a human RT² ProfilerTM PCR Array (SABiosciences) which contained primers for the detection of 84-different known angiogenic genes. This analysis was carried out according to the manufacturer's instructions. Briefly, sub-confluent 3.5 cm² dishes of HeLa cells were treated for 24 h with either PBS (vehicle) or 500 nM decorin protein core in DMEM. After incubation, the cells were lysed directly in TRIzol Reagent (Invitrogen) for subsequent RNA isolation. Total RNA was reverse transcribed to cDNA using the RT² First Stand Kit (SABiosciences) followed by combination with the RT² qPCR Mastermix. This volume was evenly distributed

among two PCR Array plates. Consecutive rounds of qPCR were performed under normal thermal conditions followed by data analysis according to the above mentioned Comparative Ct method post normalization to five independent controls.

Immunofluorescence—Immunofluorescent studies was performed as described before (53,82,83). Approximately 5×10^4 HeLa cells were plated on 4-well chamber slides (BD Biosciences) and grown to full confluence in 10% FBS at 37 °C. Cells were switched to DMEM/2% FBS 2 h prior to each treatment. Slides were rinsed twice with DPBS and fixed/permeabilized with ice-cold methanol for 10 min. Subsequently slides were subjected to standard immunofluorescence protocols, and mounted with Vectashield (Vector Laboratories Inc, Burlingame, CA). Following incubation with various primary antibodies, detection was determined using goat anti-mouse IgG Alexa Fluor® 488 and goat anti-rabbit IgG Alexa Fluor® 594 (Invitrogen). Images were acquired using a Leica DM5500B microscope with Advanced Fluorescence 1.8 software (Leica Microsystems, Inc). All the images were analyzed with Adobe Photoshop CS3 (Adobe Systems, San Jose, CA). Fluorescence quantification was done with ImageJ software.

Gelatinase Zymography—Gelatinase activities were evaluated in tumor conditioned media (10 μ l) collected from HeLa cells after incubation with 500 nM decorin for a period of 24 h were quantified with 10% SDS-PAGE incorporating denatured rat tail type I collagen (Sigma) (84). The sample buffer did not contain reducing agents. Gels were washed in 2.5% v/v Triton X-100 (1 h at room temperature) and incubated overnight in 50 mM Tris HCl, pH 7.6, 0.1 mM NaCl, 10 mM CaCl₂, 0.05% Brij in the presence or absence of 20 mM EDTA (all from Sigma). Enzymatic activity was visualized as negative staining with Coomassie Brilliant Blue R-250 (Sigma) and quantified using Quantity One 1-D Analysis Software (Bio-Rad). The results of six samples per group were averaged.

Quantification of MMP Levels—The detection of total MMP-9 and MMP-2 present in tumor-conditioned medium was carried out by ELISA according to the individual kits assaying Human MMP-9 and Human MMP-2 Immunossay Quantikine Colorimetric Sandwich ELISA (R&D Systems, Minneapolis, MN) according to the manufacturer's protocol. These assays employ a quantitative sandwich ELISA technique via a monoclonal antibody specific for both the 92-kDa Pro-MMP9 (gelatinase B) as well as the 82-kDa-active MMP9. Detection of human MMP-2 (gelatinase A) via Human MMP-2 Quantikine kit was performed with a polyclonal antibody cognant for the 72-kDa MMP2. Briefly, tumor conditioned medium samples generated

by a sub-confluent six-well plate of HeLa cells, previously treated with either PBS (mock control) or decorin protein core (500 nM) for 24 h, were collected. The pre-coated plates received Assay Diluent followed by application of standard, control, and sample cell media aliquots followed by 2h incubation at 25 °C. The plates were washed extensively, incubated with the substrate for 30 min and read at 450 nm.

Evaluation of mRNA Stability—Determination of mRNA decay processes were evaluated in HeLa via pre-treatment of Actinomycin D (Sigma, St. Louis, MO) for 1 h followed by treatment (4 h) with decorin core protein (100, 500 nM). At the conclusion of the experiment, media was aspirated, cells were washed in PBS and lysed in TRIzol for RNA isolation and cDNA synthesis (see above protocol). Yielded cDNA was subsequently analyzed via qPCR (see above protocol for workflow and $\Delta\Delta C_t$ methodology) to evaluate the resulting non-steady state mRNA levels of selected target genes in the presence or absence of decorin.

MMP-9 Functional Assay—Evaluation of endogenous MMP-9 activity present in HeLa conditioned media in the absence or presence of decorin core protein (500 nM) was carried out via utilization of the SensoLyte® Plus 520 MMP-9 Assay Kit (AnaSpec, San Jose, CA) (85,86). Briefly, following the 24 h incubation with decorin, tumor conditioned DMEM was collected, filtered (0.2 μ m), and centrifuged. The supernatant was subsequently used to generate two-fold dilutions (up to and including 1:128). About 100 μ l of each dilution was added to each microplate well, which contained a pre-coated monoclonal anti-human MMP9 antibody. Pulldown (1 h at 25 °C) of endogenous MMP9 was succeeded by activation of the pro-MMP9 present only in the standard curve with 1 mM p-aminophenylmercuric acetate (APMA) for 2 h at 37 °C but not for the control or experimental samples. This allowed direct evaluation of endogenous active MMP9 in the applied samples. Next, active MMP9 activity was assayed via the addition of the synthetic MMP9 5-FAM/QXL520 FRET peptide. Following an 8-h incubation with this MMP9 substrate, end point analysis was determined by measuring the fluorescence intensity, which measures the activity of MMP9, on a BioTek Synergy 4 plate reader (BioTek Instruments, Winooski, VT) at an Em/Ex of 490/520 nm.

Tumor Xenograft Matrigel Plug Assays—Approximately 80 μ l of Matrigel™ (BD Biosciences, Bedford, MA) containing $\sim 10^6$ MDA-231(GFP+) cells and HGF (10 ng/ml), in the presence or absence of decorin (200 nM) were injected into 4 dorsal subcutaneous regions of 6 severe combined immunodeficient (SCID), nude, female mice (Charles River Lab., Malvern, PA). Mice were sacrificed 14 days

post injection and their skins were removed, fixed in 10% buffered formalin (Fisher Science, Fair Lawn, NJ), and then photographed from the inside to analyze the resulting angiogenic reaction. Quantification was achieved by ImageJ software and superimposing grids onto each photographed skin with each box of the grid representing 1 mm². Fifty, randomly-selected boxes around each Matrigel plug were analyzed by morphometry. That is, the number of times a blood vessel intersected each box was recorded for both “Matrigel+HGF” and “Matrigel+HGF+decorin”. Values were converted into μ m² and a Student’s two-sided *t* test (see below) was used to compare the values obtained from the control and experimental conditions.

Tumor Xenografts—All animal studies were approved by the Institutional Review Board of Thomas Jefferson University. For orthotopic mammary tumor xenografts, SCID female mice (Charles River Lab., Malvern, PA) were injected in the upper left mammary gland with $1-2 \times 10^6$ MDA-231(GFP+) cells. The mice were randomized once tumors were established. Half the mice received a dose of 5 mg/kg decorin protein core injected intraperitoneally every 2 days. The controls received 100 μ l PBS. On day 24, the majority of animals were sacrificed and all major organs and tumors were dissected and frozen subsequent to analysis via immunofluorescence or qPCR. HeLa xenografts were generated as described before (52).

Dot Blot Analyses of Secreted Factors—Evaluation of secreted factors was done, in part, via dot blot analysis. HeLa and MDA-231 cells were treated as described under serum free conditions (see below). Tumor cell conditioned medium was collected, filtered, briefly centrifuged and applied to the dot blot (Minifold I, Schleicher and Schuell, Keene NH) sample well plate. Constant vacuum (~ 80 mbar) was applied for 30 min to ensure attachment to the nitrocellulose membrane. Membrane was washed, and blocked overnight in 5% BSA. Incubation with primary antibody specific for the secreted factor was followed by application of an HRP-conjugated secondary antibody and subsequent visualization with ECL technique. Densitometry was performed with ImageJ software.

Quantification and Statistical Analysis—Immunoblots were quantified by scanning densitometry using ImageJ software or using the Odyssey software for the infrared-labeled secondary antibodies. All the experiments were carried out in triplicate and repeated at least three times. Results are expressed as mean \pm SEM. Statistical analysis was performed with SigmaStat for Windows version 3.10 (Systat Software, Inc., Port Richmond, CA). Significance of differences was determined by unpaired Student’s *t* test. Statistical significance was achieved with *p* < 0.05. For

quantification of immunofluorescence studies, fluorescence intensity and 3D surface plots were quantified by measuring pixels with ImageJ software as described before (52).

RESULTS

Decorin Broadly Impedes the Transcription of Pro-Angiogenic Genes and Upregulates the Expression of Angiostatic Genes—First, we determined the effects of decorin on the expression of angiogenic genes using a human RT² ProfilerTM PCR Array (SABiosciences). This PCR array platform profiles the expression of 84 key genes involved in modulating the biological processes of angiogenesis, including growth factors and their receptors, chemokines and cytokines, matrix and adhesion molecules, proteases, as well as transcription factors.

To this end, HeLa cells were treated for 24 h in the absence or presence of 500 nM decorin protein core under normoxic conditions whereupon total RNA was harvested, reverse transcribed to cDNA libraries and then applied to the cognate PCR Array plates. Normalization of raw Ct values to five endogenous controls allowed for a comparative $\Delta\Delta$ Ct analytic approach between calibrator samples (PBS control) and experimental (decorin) samples. First, only ~10% of all genes were changed: two were upregulated and six were down-regulated by decorin (Fig. 1A). Notably, *TIMP3* was induced over 4 folds by decorin and this product has been previously shown to be antiangiogenic (87). The six down-regulated genes, (Fig 1A) including hypoxia inducible factor-1 α (*HIF1A*), sphingosine 1-phosphate receptor 1 (*S1PR1*), endoglin (*ENG*), fibroblast growth factor 2 (*FGF2*), and integrin α V (*ITGAV*), all were quite interesting because all have been implicated in promoting key aspects of angiogenic signaling (88-94), with the notable exception of thrombospondin-1 (*THBS1*) which has been shown to exhibit potent anti-angiogenic activities (95,96).

Next, we validated the modulated genes using qPCR (Fig. 1B). The great majority of the transcriptional changes reported by the PCR Array were reliably reproduced. However, the expression changes for aminopeptidase-N (*ANPEP* or *CD13*) and *S1PR1* could not be reproduced and validated most likely reflecting either an exceedingly low transcript copy number or sheer lack of expression in HeLa cells. Notably, thrombospondin-1, a well-known anti-angiogenic factor (95,96) was found to be slightly downregulated in the presence of decorin (Fig. 1A). However, verification of this gene via qPCR revealed *THBS1* to be significantly upregulated by ~ 2.5 folds ($p < 0.001$, Fig. 1B). Additional pro-angiogenic gene targets found to be repressed by decorin included VEGFA and Met. Since

we normalized Ct values to endogenous *ACTB* in each sample, we conducted qPCR to ensure the expression of this housekeeping gene was not affected by exogenous decorin. Thus, after 24 h we found that *ACTB* (supplemental Fig. S1A) in HeLa was not significantly modulated by decorin (500 nM). Further, we sought to determine *ACTB* over time and demonstrate that up to 8 h in HeLa, *ACTB* mRNA levels also did not significantly change (supplemental Fig. S1B). Therefore, we conclude the changes seen in target gene expression are not a result of β -actin modulation at the mRNA level.

The expression changes were done at steady state kinetics but could alternatively represent the effects of decorin on modulating mRNA stability and/or accelerating decay processes of the target message. To address this possibility, we evaluated *VEGFA*, *HIF1A*, and *THBS1* in the presence of decorin following pretreatment with Actinomycin-D in HeLa. We found no further changes in mRNA for *VEGFA* (supplemental Fig. S1C), *HIF1A* (supplemental Fig. S1D) or *THBS1* (supplemental Fig. S1E), indicating that decorin does not modulate mRNA levels post-transcriptionally by promoting mRNA decay. We can thus conclude that the changes seen at the steady state reflect a decrease at the level of transcription.

Collectively, these expression data implicate decorin as a broad suppressor of the tumor angiogenic response by exhibiting a unique duality. It effectively represses pro-angiogenic gene targets under normoxia and simultaneously promotes the expression of various anti-angiogenic effector molecules.

Exogenous Decorin Potently Attenuates VEGFA Signaling Components—Among the downregulated genes reported in the expression analysis above, we chose to focus on the VEGFA signaling axis as it relates to tumor angiogenesis. First, we determined whether the activity of decorin could be generalized to normal as well as transformed cells. Thus, we tested two tumor cell lines and normal endothelial cells for the effects of exogenous decorin on VEGFA production. Following decorin exposure, we found a uniform reduction of secreted VEGFA in the media conditioned for 24 h by HeLa (cervical carcinoma) and MDA-231 (triple-negative breast carcinoma) cells as well as from HUVECs ($p < 0.001$, Fig. 2 A,B).

The reduced levels of VEGFA found in the conditioned medium could be a consequence of a corresponding decrease in total cellular stores of VEGFA or an inhibitory effect of VEGFA secretion. To differentiate among these possibilities, we probed the cell lysates using immunoblotting with the same anti-VEGFA antibody. We found a decrease in cellular VEGFA in both HeLa and MDA-231 and to a lesser

extent in HUVECs ($p < 0.001$ and $p < 0.01$, respectively, Fig. 2C, D). The difference in sensitivities among these cell lines are attributable to higher Met in HeLa and MDA-231 (6- and 8-folds higher, respectively) relative to HUVEC (data not shown). Enhanced expression of this high-affinity receptor would further sensitize the cells to the angiostatic properties of decorin.

Next, we found a significant reduction of both secreted and cellular VEGFA (supplemental Fig. S2A,B) after 24h in HeLa and MDA-231 following decorin treatment (100 nM). Thus, a concentration of 100 nM is sufficient to evoke reduction of secreted and cellular VEGFA.

Time course experiments utilizing HeLa cell lysates treated with a constant concentration of decorin revealed a progressive decrease of both secreted (Fig. 2E,F) and cellular VEGFA (supplemental Fig. S2C) relative to mock (PBS) treated controls for up to 12 h. Downregulation of secreted and cellular VEGFA was noted as early as 2 h (*cfr.* Fig. 2F and S2C); thus, we conducted a VEGFA time course and found a gradual reduction of VEGFA mRNA persisting for up to 8 h in HeLa (supplemental Fig. S2D). Furthermore, immunofluorescent analysis confirmed reduction of cellular VEGFA in HeLa cells following decorin treatment (supplemental Fig. S2E).

Interestingly, cellular VEGFA levels maintained a stable decrease starting at 8 h and lasting for up to 24 h, which mirrored VEGFA expression. However, secreted VEGFA seemed to have a sharper decrease at later time points, potentially implicating an attenuation of the secretory pathway.

Collectively, our findings indicate that decorin affects VEGFA production in both transformed and normal cells and further corroborate the marked transcriptional inhibition obtained under normal oxygen tension. Moreover, these data postulate a firm role for decorin as a negative regulator of VEGFA by inhibiting its expression at multiple levels of control.

Decorin Suppresses VEGFA in the Presence of Constitutively-active HIF-1 α under Normoxic Conditions—Further interrogation behind the mechanism of decorin-mediated suppression of VEGFA signaling led us to evaluate the role of HIF-1 α based on the potent inhibition of *HIF1A* transcription under normoxic conditions (*cfr.* Fig. 1). The *HIF1A* gene encodes a key basic-helix-loop-helix transcription factor that dimerizes with the constitutively expressed HIF-1 β /ARNT subunit to form a stable complex capable of recruiting transcriptional co-activators such as CBP/p300 to proximal promoters (97). Consequently, the genetic subsets targeted by HIF-1 α are primarily responsible for orchestrating and executing the cellular hypoxic response that will drive angiogenesis. It is well

established that VEGFA expression is transcriptionally driven by HIF-1 α (89,98).

Utilization of specific MDA-231(GFP+) cell lines, which overexpress either wild-type HIF-1 α (MDA-231 wtHIF-1 α) or a mutated HIF-1 α (MDA-231 mutHIF-1 α) allowed for direct evaluation of HIF-1 α function in normoxia. In the HIF-1 α mutant, the proline residues residing within the oxygen-dependent degradation domain have been mutated to alanine (P402A and P564A) that culminate in a constitutively-active HIF-1 α . This form is no longer a proper substrate for PHD2-mediated hydroxylation and subsequent protein Von Hippel-Lindau (pVHL)-dependent ubiquitination leading to proteasomal degradation. Thus, activated HIF-1 α is stable under normoxic conditions (78). We discovered that decorin evoked downregulation of both wild-type and mutant HIF-1 α (Fig. 3A,B). Immunofluorescence detection of both HIF-1 α and VEGFA showed a significant decrease in both wild-type and mutant cells (Fig. 3C,D). We found that secreted VEGFA was also reduced in the two cell types (Fig. 3E), further supporting the data presented above. Thus, decorin evokes downregulation of HIF-1 α protein in mammary carcinoma cells harboring either wild-type or a constitutively-active HIF-1 α .

Consistent with this notion, pVHL, the E3-ubiquitin ligase complex liable for degrading HIF-1 α under normoxic conditions (99) was upregulated nearly two folds in MDA-231wtHIF-1 α , but was unchanged in MDA-231mutHIF-1 α (supplemental Fig. S3A) following increasing concentrations of decorin. Further evaluation of pVHL in parental MDA-231 cells demonstrated a modest induction (supplemental Fig. S3B); however, this was in contrast to the nearly 40% inhibition of HIF-1 α protein after 4 h (supplemental Fig. S3B), which is consistent with the above findings. Of note, treatment of HeLa demonstrated a similar trend of modestly induced pVHL correlating with reduced HIF-1 α (not shown).

Collectively, these data posit a potential role of pVHL, in conjunction with the already declining *HIF1A* expression levels, for the early stages of HIF-1 α antagonism. Therefore, inhibition of HIF-1 α does not seem to rely as heavily on pVHL, instead decorin evokes a prominent transcriptional repression. This provides a novel role of attenuating traditional HIF-1 α /VEGFA signaling under normoxic conditions to curb tumor growth.

Decorin Disables an Array of Activating Transcription Factors Essential for the Proper Expression of HIF1A and VEGFA Under Normoxia—To further investigate the potential mechanism of decorin antiangiogenic activity, we performed a detailed

expression analysis of pertinent transcription factors essential for driving the expression of both *HIF1A* and *VEGFA*. Multiple transcription factors are known to have consensus binding sites within the promoter of *VEGFA*, in particular numerous sites are present for Sp1 and AP-1 as well as a HIF-1 α response element (HRE) (89). Coincidentally, these factors are also essential for promoting and allowing *HIF1A* expression.

Taking this information into account we evaluated *FOS* and *SP1* expression within muthIF-1 α cells 4 h and 24 h post exposure to decorin. The expression of *FOS* was significantly decreased at both time points ($p < 0.001$ and $p < 0.01$, Fig 3F,G), with a greater reduction occurring after 4h with some recovery after 24 h. A similar expression signature was obtained with *SP1* at both 4 and 24 h ($p < 0.001$, 3F,G).

Next, *CTNNB1* (β -catenin) expression exhibited a reduction ($p < 0.001$, Fig. 3F) following 4h; however, after 24h, *CTNNB1* expression seemed to recover significantly (Fig. 3G), and return almost to baseline ($p < 0.05$, Fig. 3G). These data are congruent with the finding of seven TCF/LEF binding sites embedded within the proximal promoter of *VEGFA* (100) and thus enforce the critical role of β -catenin signaling in the promotion of *VEGFA*-mediated tumor angiogenesis. Further, the expression of *HIF1A* decreased significantly at 4h ($p < 0.01$, 3F) and this was protracted for up to 24 h ($p < 0.001$, 3G). Finally, in regard to *VEGFA* expression, both time points revealed a potent suppression in MDA-231 muthIF-1 α cells ($p < 0.001$, Fig. 3F,G). Overall, these expression data corroborate the above-mentioned protein and immunofluorescence data.

In summary, these data argue for a role of decorin in promoting a cessation of pro-angiogenic transcription via a potent reduction in multiple genes necessary for the expression of *HIF1A* and *VEGFA*. More importantly is the ability of decorin to achieve potent angiostasis in an activated HIF-1 α cell line under normoxic conditions. Further, classical Ras/MAPK signaling cascades emanating from RTKs such as Met (see below), are known to target and phosphorylate Sp1 via the p42/p44 MAPK, resulting in full activation and specific targeting of Sp1 to the proximal promoter of *VEGFA* for competent transactivation (101).

The role of Met in Regulating Angiogenesis vis-à-vis VEGFA Signaling—We have previously shown that binding of decorin to Met is oppositional and subsequent receptor internalization and degradation ensues (52). Therefore, focusing on the prevalent association of Met in the process of tumor angiogenesis and the documented interaction with decorin, we determined the link of Met in the process of decorin-mediated angiostasis. This link was established via the

transfection of a cocktail of three validated siRNAs targeting Met mRNA. We reasoned that Met downregulation at the mRNA level would mimic the proteasomal-induced degradation of Met evoked by exogenous decorin.

The siRNA targeting Met reduced the receptor to barely detectable levels without affecting β -actin levels (Fig. 4A). Importantly, knockdown of Met recapitulated the downregulation of cellular *VEGFA* (Fig. 4B). Furthermore, dual treatment of HeLa cells with both targeting siRNA followed by a 24 h incubation with decorin did not result in additional inhibition of cellular *VEGFA*, in agreement with Met acting as the main signaling receptor for decorin-evoked inhibition of *VEGFA* (Fig. 4B).

As discussed above, decorin suppresses the transcription of targets critical for the promotion of angiogenesis. Therefore, to dissect if decorin is transducing these anti-angiogenic effects via Met, we used siRNA targeting Met. This strategy achieved Met transcript reduction by ~50% (Fig. 4C), relative to the scrambled siRNA control. Interestingly, depletion of Met alone induced transcriptional changes in *VEGFA* and *CTNNB1* analogous to decorin-treated HeLa cells (Fig. 4C,E), but to a lesser degree. Finally, *MYC* a downstream target of the Met/ β -catenin antagonism (52), was found to change only modestly (Fig. 4C).

Surprisingly, *HIF1A* expression was not appreciably affected under these conditions (Fig. 4C). Several reasons could account for this discrepancy such as the requirement of decorin to evoke changes in *HIF1A* expression vis-à-vis Met engagement, compensatory mechanisms mediated via HIF-2 α , or because signaling is being integrated by decorin over multiple RTKs, such as the EGFR.

As a primary downstream effector of Met (52), β -catenin was prominently reduced via decorin (Fig. 4 D). This inhibition also extended to *CTNNB1* transcripts (Fig. 4E), to an extent comparable to MDA-231 wtHIF-1 α as shown previously (*cfr.* Fig. 3F). As decorin downregulates Met protein levels via caveolar-mediated endocytosis and proteasomal-dependent degradation (47), we tested the effects of decorin on *MET* transcript levels. Notably, we found a significant reduction in the expression of *MET* (*cfr.* Fig. 1B) indicating disruption of a positive feedback loop that exists between Met and β -catenin upon decorin engagement (102). It is tempting to speculate that decorin is abrogating both β -catenin and Sp1 signaling subsequent to Met degradation, resulting in transcriptional inhibition of the *VEGFA* locus. Importantly, this fosters a scenario wherein a growth factor receptor dependent mechanism of HIF-1 α regulation is feasible, and is congruent with the

biological activity decorin exerts on Met (103). Notably, decorin-null mice have increased expression of β -catenin in the enteric epithelium (57).

Further proof-of-principle of decorin mediated angiostasis was established by employing a tumor xenograft mouse Matrigel assay. To this end, we injected $\sim 10^6$ MDA-231 (GFP+) cells mixed with ~ 80 μ l of Matrigel and 10 ng/ml HGF in the absence or presence of decorin (200 nM) into four dorsal subcutaneous regions of SCID mice. After 14 days with HGF, a strong angiogenic reaction was achieved surrounding the tumors (asterisk, Fig. 4F, left panel). This is in stark contrast to the combined treatment of decorin and HGF for the same time period (asterisk, Fig. 4F, right panel). Morphometric analysis of the vessel density revealed a marked suppression of vascularity associated with the decorin-containing xenografts ($p < 0.001$, Fig. 4G).

These *in vivo* findings argue a very strong case for the ability of decorin to retard tumor angiogenesis in MDA-231 tumor xenograft Matrigel assays. These data establish and enforce a role of Met as being involved in a non-canonical Wnt/ β -catenin signaling pathway induced by HGF to promote tumor angiogenesis vis-à-vis VEGFA, which can be abrogated by decorin.

Decorin Inhibits the Induction and Activity of Matrix Metalloproteinases—Aggressive neoplasms often show increased expression of a class of zinc-dependent gelatinases known as matrix metalloproteases (MMPs) capable of degrading the matrix as well as liberating a host of pro-angiogenic factors (104,105). Primarily pertinent for the current study is the ability of matrix-bound VEGFA to be released, making the factor readily available for use by the surrounding angiogenic cells (106). Taking this into account, we analyzed the expression and activity of MMP9 and MMP2, both of which are under the control of β -catenin signaling (107). MMPs are secreted by the host cell as a zymogen (otherwise known as the “proform”), followed by a proteolytic cleavage event to yield the catalytically active enzyme. Thus, to assess the activity of secreted MMPs, media conditioned for 24 h by HeLa cells in the absence or presence of exogenous decorin (500 nM) were subjected to gelatin zymography. This functional assay revealed a dramatic reduction in the activity of MMP9 as well as a more modest, but still significant, decrease in the activity of MMP2 (Fig. 5A) relative to control conditioned media ($p < 0.001$ and $p < 0.05$, respectively, Fig. 5B). In agreement with gel zymography, utilization of a MMP9 fluorescence resonance energy transfer (FRET) probe assay revealed $>50\%$ reduction in the activity of endogenous MMP9 present in HeLa conditioned media following decorin treatment (Fig. 5C). In support of these functional data,

gene expression analysis revealed an effective decrease in MMP9 ($p < 0.001$, Fig. 5D) and a modest but statistically significant reduction in MMP2 ($p < 0.05$, Fig. 5D). We then performed ELISA with antibodies specific for both MMPs and showed a significant decrease in secreted MMP9 ($p < 0.001$, Fig. 5E) without any significant reduction in secreted MMP2 (Fig. 5F). These data are uniformly consistent with the gelatin zymography and gene expression data presented above.

Next, we evaluated the role of a membrane type MMP, known as MT1-MMP (or MMP14) which pro-angiogenic and pro-invasive via the cleavage and activation of MMP2 and MMP9 (108,109). To this end, we carried out immunoblotting to detect MT1-MMP in our HeLa samples and subsequently found no significant change in MT1-MMP levels (Fig. 5G). We also found no appreciable changes in the expression of MMP14 (not shown).

Collectively, these data indicate that decorin is most likely not attenuating MMP2/9 activity or expression via modulation of a presumed upstream activator, i.e. MT1-MMP. Moreover, these data provide further evidence for the potent transcriptional control decorin exerts over these loci by abrogating non-canonical β -catenin signaling.

Finally we evaluated the role of TIMP3, a secreted protein that binds tightly to the extracellular matrix and is also a direct inhibitor of ADAM-17/TACE (110). TIMP3 has also been proposed to be a tumor suppressor in several human cancers such as kidney, colon, brain, meningiomas, and non-small cell lung cancers (111–113). Interestingly, TIMP3 has also been reported to reduce Met receptor shedding (114). According to the array (*cfr.* Fig. 1), decorin induces TIMP3 expression; thus, we evaluated HeLa cell conditioned media and found an almost 5-fold increase in secreted TIMP3 (supplemental Fig. S4A). Further, immunofluorescent analysis of MDA-231(GFP+) tumor xenograft cyrosections also revealed an abundant increase in TIMP3 signal intensity (supplemental Fig. S4B), thus indicating a decorin-dependent induction of TIMP3 *in vitro* and *in vivo*.

We conclude that decorin suppresses the expression and functional activity of MMP2/9 at least in part by antagonizing Met signaling. This would result in a protracted degradation and inhibition of β -catenin in a non-canonical Wnt, RTK-dependent manner insofar as both MMP2 and MMP9 are direct transcriptional targets of β -catenin (107).

Decorin Induces Thrombospondin-1 both in Cell Cultures and Tumor Xenografts—Next, we determined the levels of secreted thrombospondin-1 in media conditioned by HeLa cells that were exposed to either vehicle (control) or decorin (500 nM) for 24 h. Using

quantitative dot blot analysis, we found a marked increase in the secretion of thrombospondin-1 (Fig. 6A) whereas the secretion of perlecan (internal control) was not appreciably changed (Fig. 6B). Similarly, the cellular levels of thrombospondin-1 were also significantly increased by decorin (Fig. 6C).

Next, we utilized mice bearing HeLa tumor xenografts which were treated with intraperitoneal injections of decorin (5 mg/Kg) every other day over a period of 23 days. At the end of the treatment, the volume of the decorin-treated tumors was ~half the size of vehicle-treated counterparts ($p < 0.001$, $n = 6$ per group, Fig. 6D). Immunofluorescence analysis of frozen tumor sections showed a marked induction of endogenous human thrombospondin-1 in the treated tumor xenografts (Fig. 6E). Concurrently, the amount of endogenous VEGFA was markedly reduced in the decorin-treated xenografts (supplemental Fig. S5).

Further *in vivo* relevance of decorin-mediated angiostasis was determined via qPCR to evaluate the expression of pro-angiogenic markers present in the tumor xenografts. In the treated xenografts, there was a substantial downregulation of *MMP2*, *MMP9* and *VEGFA* ($p < 0.001$, Fig. 6F) and a marked upregulation (up to 15 folds) of *THBS1* ($p < 0.001$, Fig. 6G) transcription.

Overall, these data correlate well with the *in vitro* findings and further strengthen the concept and current rationale while providing a proof-of-principle for decorin-mediated inhibition of VEGFA-mediated tumor angiogenesis.

Systemic Administration of Decorin Inhibits Pro-angiogenic Markers in Orthotopic Tumor Xenografts — To further strengthen the *in vivo* relevance of our data, we generated orthotopic mammary tumor xenografts using triple-negative breast carcinoma cells MDA-231(GFP+). In this case, systemic treatment with decorin protein core resulted in a marked induction of endogenous human thrombospondin-1 by systemic delivery of decorin (supplemental Fig. S6A). In addition, the HeLa xenografts demonstrated an almost complete loss of cellular VEGFA within the decorin treated cohort relative to control animals when analyzed via immunofluorescence and quantified as 3D surface plots of the fluorescent signal (supplemental Fig. S6B). Collectively, our results indicate that decorin can simultaneously downregulate proangiogenic factors and upregulate antiangiogenic factors in two animal models of tumorigenesis.

DISCUSSION

The steps involved in tumor progression have been derived from multiple animal models and reflect discrete changes within the genome via activation of

oncogenes or the silencing of tumor suppressor genes that drive a normal cell through transformation to a malignant phenotype (115). A key milestone on the path to cancer progression is the development of a competent tumor vasculature to provide a blood supply as well as a conduit for metastasis. This event is mediated via a discrete step known as the angiogenic switch, which results in an imbalance of key pro-angiogenic cytokines and angiogenic inhibitors. Previous reports implicate decorin as a powerful inhibitor of tumor angiogenesis (73). In our current working model (Fig. 7) stromal decorin engages and abrogates the HGF/Met signaling axis, acting as a potent suppressor of VEGFA-mediated tumor angiogenesis. Decorin binding to Met initiates receptor internalization via increased phosphorylation of Tyr¹⁰⁰³, which is a recruitment site for the E3 ubiquitin ligase c-Cbl. This mechanism triggers caveolar-mediated endocytosis of the receptor complex, culminating in the transcriptional repression of HIF-1 α , β -catenin, MYC, and SP1 under normoxic conditions, coincident with decreased protein levels and proteasomal degradation of HIF-1 α , β -catenin, and MYC (Fig. 7). The combinatorial effect of inhibiting this constellation of transcription factors results in the impairment of *VEGFA*, *MMP2*, and *MMP9* expression, and a simultaneous transcriptional induction of *THBS1* and *TIMP3*, potent inhibitors of angiogenesis and the MMP family. Moreover, we envisage that a concurrent reduction of MMP2/9 activity coupled with induction of thrombospondin-1 and TIMP3 allows for potent angiostasis in the matrix, acting to further restrict matrix-bound VEGFA from engaging cognate receptors (e.g. VEGF-R2) on the surface of tumor endothelial cells (Fig. 7). The potential involvement of MT1-MMP (MMP14) was evaluated and found to be unchanged since this membrane type MMP is postulated to orchestrate several steps directly during cancer progression including the degradation of physical barriers (e.g. laminin-5) necessary for cancer cell invasion (invadopodia), migration, activation of TGF- β , and indirectly for tumor angiogenesis through cleavage and activation of pro-angiogenic MMP2 and MMP9, at the cell surface. MT1-MMP has also been reported to remodel the basement membrane and regulate cell proliferation during renal development (116).

Notably, thrombospondin-1 expression is negatively regulated by Myc (117,118), thereby allowing establishment of the angiogenic switch and tumor progression, particularly of mammary epithelial cells (119). Thus, an additional way through which decorin could induce thrombospondin-1 would be via repression of Myc (52). Moreover, HGF induces a severe repression of *THBS1* expression via activation of Met (77). Thus, interference of the HGF/Met signaling axis,

as coordinated by decorin, not only serves to repress VEGFA but also acts to potentially induce thrombospondin-1, further preventing Met and VEGFA mediated tumor angiogenesis.

We previously reported that stable expression of decorin in several malignant cell lines led to inhibition of endogenous VEGFA expression (73). However, the mechanism of this effect was not investigated. In the present study we have expanded these original observations and unmasked a mechanism that is controlled by a decorin-evoked downregulation of Met, and perhaps other RTKs. An additional novelty of this current study lies in the identification of a normoxic and HIF-1 α -dependent mechanism as a molecular basis for these findings. Furthermore, at the time of publication of our previous study, we were unaware of the recently-established high affinity interaction of decorin with the pro-angiogenic Met receptor (51). Abrogating the EGFR activity by functionally blocking the receptor with mAb425 or utilizing AG1478, in the presence of decorin was able to evoke rapid activation of Met followed by internalization and downregulation of total Met levels, implicating Met as the primary receptor for decorin. Finally, it was subsequently found that Met has a substantially higher affinity for decorin relative to that of EGFR (51).

This angiostatic effect has probable implications that attenuate the initial stages of tumor angiogenesis. In this phase, which precedes the activation of the angiogenic switch, tumor hypoxia has not yet reached a biologically relevant threshold to induce tumor vascularization. This delineates a compelling role for matrix-derived residents as being essential modulators of early angiogenic events.

Our data presented here seemingly contradicts with a previously published study (120) which reported that decorin is able to induce VEGF production by recruiting Sp1, HIF-1 α , and STAT3 to the cognizant response elements within the promoter of *VEGF*. This study, however, was performed with murine cerebral endothelial cells (120). Our study, in contrast, was conducted in two human carcinoma cell lines. In this context, the molecular repertoire and genomic profile of malignant human cervical and breast cell lines compared to normal mouse cerebral endothelial cells make comparison difficult. Further, our data concerning the effect of decorin for normal human endothelial cells suggest an inhibitory role, which is supported by a recent study demonstrating decorin antagonizes VEGFR2 in human extravillous trophoblasts and interfering with migration by attenuating ERK1/2 signaling (121).

In conclusion, our data demonstrate a novel antagonistic interaction of the HGF-Met signaling axis leading to a marked and sustainable inhibition of VEGFA-mediated angiogenesis under normoxic conditions. Potential therapeutic induction of this mechanism of decorin, acting as a potent angiostatic agent, will attenuate critical steps in the progression of a malignant neoplasm and will have broad medicinal applications as an angiostatic modality.

Acknowledgements—We thank Nutan Pal for help in the initial stages of this project.

REFERENCES

1. Bissell, M. J. and Hines, W. C. (2011) *Nat.Med.* **17**, 320-329
2. Ferrara, N. and Kerbel, R. S. (2005) *Nature* **438**, 967-974
3. Iozzo, R. V. (1998) *Annu.Rev.Biochem.* **67**, 609-652
4. Iozzo, R. V. (2005) *Nat.Rev.Mol.Cell Biol.* **6**, 646-656
5. Iozzo, R. V. and Sanderson, R. D. (2011) *J.Cell.Mol.Med.* **15**, 1013-1031
6. Iozzo, R. V. and Murdoch, A. D. (1996) *FASEB J.* **10**, 598-614
7. Iozzo, R. V. (1999) *J.Biol.Chem.* **274**, 18843-18846
8. Schaefer, L. and Iozzo, R. V. (2008) *J.Biol.Chem.* **283**, 21305-21309
9. Danielson, K. G., Baribault, H., Holmes, D. F., Graham, H., Kadler, K. E., and Iozzo, R. V. (1997) *J.Cell Biol.* **136**, 729-743
10. Reed, C. C. and Iozzo, R. V. (2002) *Glycoconj.J.* **19**, 249-255
11. Keene, D. R., San Antonio, J. D., Mayne, R., McQuillan, D. J., Sarris, G., Santoro, S. A., and Iozzo, R. V. (2000) *J.Biol.Chem.* **275**, 21801-21804
12. Zhang, G., Ezura, Y., Chervoneva, I., Robinson, P. S., Beason, D. P., Carine, E. T., Soslowsky, L. J., Iozzo, R. V., and Birk, D. E. (2006) *J.Cell.Biochem.* **98**, 1436-1449
13. Zhang, G., Chen, S., Goldoni, S., Calder, B. W., Simpson, H. C., Owens, R. T., McQuillan, D. J., Young, M. F., Iozzo, R. V., and Birk, D. E. (2009) *J.Biol.Chem.* **284**, 8888-8897

14. Rühland, C., Schönherr, E., Robenek, H., Hansen, U., Iozzo, R. V., Bruckner, P., and Seidler, D. G. (2007) *FEBS J.* **274**, 4246-4255
15. Sanches, J. C. T., Jones, C. J. P., Aplin, J. D., Iozzo, R. V., Zorn, T. M. T., and Oliveira, S. F. (2010) *J.Anat.* **216**, 144-155
16. Kalamajski, S. and Oldberd, Å. (2010) *Matrix Biol.* **29**, 248-253
17. Robinson, P. S., Lin, T. W., Jawad, A. F., Iozzo, R. V., and Soslowsky, L. J. (2004) *Ann.Biomed.Eng.* **32**, 924-931
18. Robinson, P. S., Huang, T. F., Kazam, E., Iozzo, R. V., Birk, D. E., and Soslowsky, L. J. (2005) *J.Biomechanical Eng.* **127**, 181-185
19. Fust, A., LeBellego, F., Iozzo, R. V., Roughley, P. J., and Ludwig, M. S. (2005) *Am.J.Physiol.Lung Cell Mol.Physiol.* **288**, L159-L166
20. Ferdous, Z., Wei, V. M., Iozzo, R. V., Höök, M., and Grande-Allen, K. J. (2007) *J.Biol.Chem.* **282**, 35887-35898
21. Elliott, D. M., Robinson, P. S., Gimbel, J. A., Sarver, J. J., Abboud, J. A., Iozzo, R. V., and Soslowsky, L. J. (2003) *Ann.Biomed.Eng.* **31**, 599-605
22. Järveläinen, H., Puolakkainen, P., Pakkanen, S., Brown, E. L., Höök, M., Iozzo, R. V., Sage, H., and Wight, T. N. (2006) *Wound Rep.Reg.* **14**, 443-452
23. Baghy, K., Dezsó, K., László, V., Fullár, A., Péterfia, B., Paku, S., Nagy, P., Schaff, Z., Iozzo, R. V., and Kovalszky, I. (2011) *Lab.Invest.* **91**, 439-451
24. Brown, E. L., Wooten, R. M., Johnson, B. J., Iozzo, R. V., Smith, A., Dolan, M. C., Guo, B. P., Weis, J. J., and Höök, M. (2001) *J.Clin.Invest.* **107**, 845-852
25. Liang, F. T., Wang, T., Brown, E. L., Iozzo, R. V., and Fikrig, E. (2004) *Am.J.Pathol.* **165**, 977-985
26. Goldberg, M., Septier, D., Rapoport, O., Iozzo, R. V., Young, M. F., and Ameye, L. G. (2005) *Calcif.Tissue.Int.* **77**, 297-310
27. Haruyama, N., Sreenath, T. L., Suzuki, S., Yao, X., Wang, Z., Wang, Y., Honeycutt, C., Iozzo, R. V., Young, M. F., and Kulkarni, A. B. (2009) *Matrix Biol.* **28**, 129-136
28. Corsi, A., Xu, T., Chen, X.-D., Boyde, A., Liang, J., Mankani, M., Sommer, B., Iozzo, R. V., Eichstetter, I., Robey, P. G., Bianco, P., and Young, M. F. (2002) *J.Bone Miner.Res.* **17**, 1180-1189
29. Brandan, E., Cabello-Verrugio, C., and Vial, C. (2008) *Matrix Biol.* **27**, 700-708
30. Zoeller, J. J., Pimtong, W., Corby, H., Goldoni, S., Iozzo, A. E., Owens, R. T., Ho, S.-Y., and Iozzo, R. V. (2009) *J.Biol.Chem.* **284**, 11728-11737
31. Bi, Y., Stuelten, C. H., Kilts, T., Wadhwa, S., Iozzo, R. V., Robey, P. G., Chen, X.-D., and Young, M. F. (2005) *J.Biol.Chem.* **280**, 30481-30489
32. Weis, S. M., Zimmerman, S. D., Shah, M., Covell, J. W., Omens, J. H., Ross, J., Jr., Dalton, N., Jones, Y., Reed, C. C., Iozzo, R. V., and McCulloch, A. D. (2005) *Matrix Biol.* **24**, 313-324
33. Chen, S., Sun, M., Meng, X., Iozzo, R. V., Kao, W. W. Y., and Birk, D. E. (2011) *Am.J.Pathol.* **179**, 2409-2419
34. Schaefer, L., Macakova, K., Raslik, I., Micegova, M., Gröne, H.-J., Schönherr, E., Robenek, H., Echtermeyer, F. G., Grässel, S., Bruckner, P., Schaefer, R. M., Iozzo, R. V., and Kresse, H. (2002) *Am.J.Pathol.* **160**, 1181-1191
35. Schaefer, L., Mihalik, D., Babelova, A., Krzyzankova, M., Grone, H. J., Iozzo, R. V., Young, M. F., Seidler, D. G., Lin, G., Reinhardt, D., and Schaefer, R. M. (2004) *Am.J.Pathol.* **165**, 383-396
36. Schaefer, L., Tsalastra, W., Babelova, A., Baliova, M., Minnerup, J., Sorokin, L., Gröne, H.-J., Reinhardt, D. P., Pfeilschifter, J., Iozzo, R. V., and Schaefer, R. M. (2007) *Am.J.Pathol.* **170**, 301-315
37. Williams, K. J., Qiu, G., Usui, H. K., Dunn, S. R., McCue, P., Bottinger, E., Iozzo, R. V., and Sharma, K. (2007) *Am.J.Pathol.* **171**, 1441-1450
38. Schaefer, L. (2011) *J.Am.Soc.Nephrol.* **22**, 1200-1207
39. Merline, R., Moreth, K., Beckmann, J., Nastase, M. V., Zeng-Brouwers, J., Tralhão, J. G., Lemarchand, P., Pfeilschifter, J., Schaefer, R. M., Iozzo, R. V., and Schaefer, L. (2011) *Sci.Signal.* **4**, ra75
40. Iozzo, R. V., Bolender, R. P., and Wight, T. N. (1982) *Lab.Invest.* **47**, 124-138
41. Adany, R., Heimer, R., Caterson, B., Sorrell, J. M., and Iozzo, R. V. (1990) *J.Biol.Chem.* **265**, 11389-11396
42. Iozzo, R. V., Moscatello, D., McQuillan, D. J., and Eichstetter, I. (1999) *J.Biol.Chem.* **274**, 4489-4492

43. Moscatello, D. K., Santra, M., Mann, D. M., McQuillan, D. J., Wong, A. J., and Iozzo, R. V. (1998) *J.Clin.Investig.* **101**, 406-412
44. Csordás, G., Santra, M., Reed, C. C., Eichstetter, I., McQuillan, D. J., Gross, D., Nugent, M. A., Hajnóczky, G., and Iozzo, R. V. (2000) *J.Biol.Chem.* **275**, 32879-32887
45. Santra, M., Reed, C. C., and Iozzo, R. V. (2002) *J.Biol.Chem.* **277**, 35671-35681
46. Santra, M., Eichstetter, I., and Iozzo, R. V. (2000) *J.Biol.Chem.* **275**, 35153-35161
47. Santra, M., Skorski, T., Calabretta, B., Lattime, E. C., and Iozzo, R. V. (1995) *Proc.Natl.Acad.Sci.USA* **92**, 7016-7020
48. De Luca, A., Santra, M., Baldi, A., Giordano, A., and Iozzo, R. V. (1996) *J.Biol.Chem.* **271**, 18961-18965
49. Santra, M., Mann, D. M., Mercer, E. W., Skorski, T., Calabretta, B., and Iozzo, R. V. (1997) *J.Clin.Invest.* **100**, 149-157
50. Patel, S., Santra, M., McQuillan, D. J., Iozzo, R. V., and Thomas, A. P. (1998) *J.Biol.Chem.* **273**, 3121-3124
51. Goldoni, S., Humphries, A., Nyström, A., Sattar, S., Owens, R. T., McQuillan, D. J., Ireton, K., and Iozzo, R. V. (2009) *J.Cell Biol.* **185**, 743-754
52. Buraschi, S., Pal, N., Tyler-Rubinstein, N., Owens, R. T., Neill, T., and Iozzo, R. V. (2010) *J.Biol.Chem.* **285**, 42075-42085
53. Zhu, J.-X., Goldoni, S., Bix, G., Owens, R. A., McQuillan, D., Reed, C. C., and Iozzo, R. V. (2005) *J.Biol.Chem.* **280**, 32468-32479
54. Kermorgant, S. and Parker, P. J. (2005) *Cell Cycle* **4**, 352-355
55. Liu, Z.-X., Yu, C. F., Nickel, C., Thomas, S., and Cantley, L. G. (2002) *J.Biol.Chem.* **277**, 10452-10458
56. Iozzo, R. V., Chakrani, F., Perrotti, D., McQuillan, D. J., Skorski, T., Calabretta, B., and Eichstetter, I. (1999) *Proc.Natl.Acad.Sci.USA* **96**, 3092-3097
57. Bi, X., Tong, C., Dokendorff, A., Banroft, L., Gallagher, L., Guzman-Hartman, G., Iozzo, R. V., Augenlicht, L. H., and Yang, W. (2008) *Carcinogenesis* **29**, 1435-1440
58. Reed, C. C., Gauldie, J., and Iozzo, R. V. (2002) *Oncogene* **21**, 3688-3695
59. Tralhão, J. G., Schaefer, L., Micegova, M., Evaristo, C., Schönherr, E., Kayal, S., Veiga-Fernandes, H., Danel, C., Iozzo, R. V., Kresse, H., and Lemarchand, P. (2003) *FASEB J.* **17**, 464-466
60. Reed, C. C., Waterhouse, A., Kirby, S., Kay, P., Owens, R. A., McQuillan, D. J., and Iozzo, R. V. (2005) *Oncogene* **24**, 1104-1110
61. Seidler, D. G., Goldoni, S., Agnew, C., Cardi, C., Thakur, M. L., Owens, R. A., McQuillan, D. J., and Iozzo, R. V. (2006) *J.Biol.Chem.* **281**, 26408-26418
62. Zafiropoulos, A., Nikitovic, D., Katonis, P., Tsatsakis, A., Karamanos, N. K., and Tzanakakis, G. N. (2008) *Mol.Cancer.Res.* **6**, 785-794
63. Goldoni, S., Seidler, D. G., Heath, J., Fassan, M., Baffa, R., Thakur, M. L., Owens, R. A., McQuillan, D. J., and Iozzo, R. V. (2008) *Am.J.Pathol.* **173**, 844-855
64. Li, X., Pennisi, A., and Yaccoby, S. (2008) *Blood* **112**, 159-168
65. Hu, Y., Sun, H., Owens, R. T., Wu, J., Chen, Y. Q., Berquin, I. M., Perry, D., O'Flaherty, J. T., and Edwards, I. J. (2009) *Neoplasia* **11**, 1042-1053
66. Nelimarkka, L., Kainulainen, V., Schönherr, E., Moisander, S., Jortikka, M., Lammi, M., Elenius, K., Jalkanen, M., and Järveläinen, H. T. (1997) *J.Biol.Chem.* **272**, 12730-12737
67. Nelimarkka, L., Salminen, H., Kuopio, T., Nikkari, S., Ekfors, T., Laine, J., Pelliniemi, L., and Järveläinen, H. (2001) *Am.J.Pathol.* **158**, 345-353
68. Schönherr, E., Levkau, B., Schaefer, L., Kresse, H., and Walsh, K. (2001) *J.Biol.Chem.* **276**, 40687-40692
69. Schönherr, E., Sunderkotter, C., Schaefer, L., Thanos, S., Grässel, S., Oldberg, Å., Iozzo, R. V., Young, M. F., and Kresse, H. (2004) *J.Vasc.Res.* **41**, 499-508
70. Kinsella, M. G., Fischer, J. W., Mason, D. P., and Wight, T. N. (2000) *J.Biol.Chem.* **275**, 13924-13932
71. de Lange Davies, C., Melder, R. J., Munn, L. L., Mouta-Carreira, C., Jain, R. K., and Boucher, Y. (2001) *Microvasc.Res.* **62**, 26-42
72. Mohan, R. R., Tovey, J. C. K., Sharma, A., Schultz, G., Cowden, J. W., and Tandon, A. (2011) *PLoS ONE* **6**, e26432
73. Grant, D. S., Yenisey, C., Rose, R. W., Tootell, M., Santra, M., and Iozzo, R. V. (2002) *Oncogene* **21**, 4765-4777

74. Salomäki, H. H., Sainio, A. O., Söderström, M., Pakkanen, S., Laine, J., and Järveläinen, H. T. (2008) *J.Histochem.Cytochem.* **56**, 639-646
75. Lai, A. Z., Abella, J. V., and Park, M. (2009) *Trends Cell Biol.* **19**, 542-551
76. Grant, D. S., Kleinman, H. K., Goldberg, I. D., Bhargava, M. M., Nickoloff, B. J., Kinsella, J. L., Polverini, P., and Rosen, E. M. (1993) *Proc.Natl.Acad.Sci.USA* **90**, 1937-1941
77. Zhang, Y.-W., Su, Y., Volpert, O. V., and Vande Woude, G. F. (2003) *Proc.Natl.Acad.Sci.USA* **100**, 12718-12723
78. Chiavarina, B., Whitaker-Menezes, D., Migneco, G., Martinez-Outschoorn, U. E., Pavlides, S., Howell, A., Tanowitz, H. B., Casimiro, M. C., Wang, C., Pestell, R. G., Grieshaber, P., Caro, J., Sotgia, F., and Lisanti, M. P. (2010) *Cell Cycle* **9**, 3534-3551
79. Cohen, I. R., Murdoch, A. D., Naso, M. F., Marchetti, D., Berd, D., and Iozzo, R. V. (1994) *Cancer Res.* **54**, 5771-5774
80. Iozzo, R. V. (1994) *Matrix Biol.* **14**, 203-208
81. Goyal, A., Pal, N., Concannon, M., Paulk, M., Doran, M., Poluzzi, C., Sekiguchi, K., Whitelock, J. M., Neill, T., and Iozzo, R. V. (2011) *J.Biol.Chem.* **286**, 25947-25962
82. Zoeller, J. J., McQuillan, A., Whitelock, J., Ho, S.-Y., and Iozzo, R. V. (2008) *J.Cell Biol.* **181**, 381-394
83. Iozzo, R. V., Buraschi, S., Genua, M., Xu, S.-Q., Solomides, C. C., Peiper, S. C., Gomella, L. G., Owens, R. T., and Morrione, A. (2011) *J.Biol.Chem.* **286**, 34712-34721
84. Hembry, R. M., Atkinson, S. J., and Murphy, G. (2007) *Methods Mol.Med.* **135**, 227-238
85. Okawa, T., Michaylira, C. Z., Kalabis, J., Stairs, D. B., Nakagawa, H., Andl, C. D., Johnstone, C. N., Klein-Szanto, A. J., El-Deiry, W. S., Cukierman, E., Herlyn, M., and Rustgi, A. K. (2007) *Genes Dev.* **21**, 2788-2803
86. Liao, S.-S., Jazag, A., and Whang, E. E. (2006) *Cancer Res.* **66**, 11613-11622
87. Bourboulia, D. and Stetler-Stevenson, W. G. (2010) *Semin.Cancer Biol.* **20**, 161-168
88. Woodfin, A., Voisin, M.-B., and Nourshargh, S. (2007) *Arterioscler.Thromb.Vasc.Biol.* **27**, 2514-2523
89. Semenza, G. L. (2002) *Biochem.Pharmacol.* **64**, 993-998
90. Avraamides, C. J., Garmy-Susini, B., and Varner, J. A. (2008) *Nat.Rev.Cancer* **8**, 604-617
91. Daum, G., Grabski, A., and Reidy, M. A. (2009) *Arterioscler Thromb Vasc.Biol.* **29**, 1439-1443
92. Rangel, R., Sun, Y., Guzman-Rojas, L., Ozawa, M. G., Sun, J., Giordano, R. J., Van Pelt, C. S., Tinkey, P. T., Behringer, R. R., Sidman, R. L., Arap, W., and Pasqualini, R. (2007) *Proc.Natl.Acad.Sci.USA* **104**, 4588-4593
93. Bernabeu, C., Lopez-Novoa, J. M., and Quintanilla, M. (2009) *Biochim.Biophys.Acta* **1792**, 954-973
94. Hynes, R. O. (2007) *J.Thromb.Haemost.* **5 (Suppl.1)**, 32-40
95. Armstrong, L. C. and Bornstein, P. (2003) *Matrix Biol.* **22**, 63-71
96. Zhang, Z. and Lawler, J. (2007) *Microvasc.Res.* **74**, 90-99
97. Pagès, G. and Pouyssegur, J. (2005) *Cardiovasc.Res.* **65**, 564-573
98. Lando, D., Peet, D. J., Whelan, D. A., Gorman, J. J., and Whitelaw, M. L. (2002) *Science* **295**, 858-861
99. Semenza, G. L. (2009) *Semin.Cancer Biol.* **19**, 12-16
100. Easwaran, V., Lee, S. H., Inge, L., Guo, L., Goldbeck, C., Garrett, E., Wiesmann, M., Garcia, P. D., Fuller, J. H., Chan, V., Randazzo, F., Gundel, R., Warren, R. S., Escobedo, J., Aukerman, S. L., Taylor, R. N., and Fantl, W. J. (2003) *Cancer Res.* **63**, 3145-3153
101. Milanini-Mongiat, J., Pouyssegur, J., and Pagès, G. (2002) *J.Biol.Chem.* **277**, 20631-20639
102. Rasola, A., Fassetta, M., De Bacco, F., D'Alessandro, L., Gramaglia, D., Di Renzo, M. G., and Comoglio, P. M. (2007) *Oncogene* **26**, 1078-1087
103. Iozzo, R. V. and Schaefer, L. (2010) *FEBS J.* **277**, 3864-3875
104. Whitelock, J. M., Murdoch, A. D., Iozzo, R. V., and Underwood, P. A. (1996) *J.Biol.Chem.* **271**, 10079-10086
105. Goldoni, S. and Iozzo, R. V. (2008) *Int.J.Cancer* **123**, 2473-2479
106. Lee, S., Jilani, S. M., Nikolova, G. V., Carpizo, D., and Iruela-Arispe, M. L. (2005) *J.Cell Biol.* **169**, 681-691
107. Wu, B., Crampton, S. P., and Hughes, C. C. W. (2007) *Immunity* **26**, 227-239
108. Zarrabi, K., Dufour, A., Li, J., Kusc, C., Pulkoski-Gross, A., Zhi, J., Hu, Y., Sampson, N. S., Zucker, S., and Cao, J. (2011) *J.Biol.Chem.* **286**, 33167-33177
109. Gialeli, C., Theocharis, A. D., and Karamanos, N. K. (2011) *FEBS J.* **278**, 16-27

110. Fata, J. E., Leco, K. J., Voura, E. B., Yu, H.-Y. E., Waterhouse, P., Murphy, G., Moorehead, R. A., and Khokha, R. (2001) *J.Clin.Invest.* **108**, 831-840
111. Bachman, K. E., Herman, J. G., Corn, P. G., Merlo, A., Costello, J. F., Cavenee, W. K., Baylin, S. B., and Graff, J. R. (1999) *Cancer Res.* **59**, 798-802
112. Barski, D., Wolter, M., Reifemberger, G., and Riemenschneider, M. J. (2010) *Brain Pathol.* **20**, 623-631
113. Zöchbauer-Müller, S., Fong, K. M., Virmani, A. K., Geradts, J., Gazdar, A. F., and Minna, J. D. (2001) *Cancer Res.* **61**, 249-255
114. Nath, D., Williamson, N. J., Jarvis, R., and Murphy, G. (2001) *J.Cell Sci.* **114**, 1213-1220
115. Hahn, W. C. and Weinberg, R. A. (2002) *N.Engl.J.Med.* **347**, 1593-1603
116. Riggins, K. S., Mernaugh, G., Su, Y., Quaranta, V., Koshikawa, N., Seiki, M., Pozzi, A., and Zent, R. (2010) *Exp.Cell Res.* **316**, 2993-3005
117. Tikhonenko, A. T., Black, D. J., and Linial, M. L. (1996) *J.Biol.Chem.* **271**, 30741-30747
118. Ngo, C. V., Gee, M., Akhtar, N., Yu, D., Volpert, O., Auerbach, R., and Thomas-Tikhonenko, A. (2000) *Cell Growth Differ.* **11**, 201-210
119. Watnick, R. S., Cheng, Y.-N., Rangarajan, A., Ince, T. A., and Weinberg, R. A. (2003) *Cancer Cell* **3**, 219-231
120. Santra, M., Santra, S., Zhang, J., and Chopp, M. (2008) *J.Neurochem.* **105**, 324-337
121. Khan, G. A., Girish, G. V., Lala, N., DiGuglielmo, G. M., and Lala, P. K. (2011) *Mol.Endocrinol.* **25**, 1431-1443

FOOTNOTES

*This work was supported in part by National Institutes of Health Grants RO1 CA39481, RO1 CA47282 and RO1 CA120975 (to R.V.I.). T. Neill was supported by NIH training grant T32 AA07463. This work is a partial fulfillment of T. Neill's doctoral thesis in Cell and Developmental Biology, Thomas Jefferson University.

²The abbreviations used are: SLRPs, small leucine-rich proteoglycans; EGFR, epidermal growth factor receptor; HGF, hepatocyte growth factor; RTK, receptor tyrosine kinase; VEGFA, vascular endothelial growth factor A; HIF-1 α , hypoxia inducible factor 1 α ; CDKI, cyclin dependent kinase inhibitor; p21, p21^{WAF1/Cip1}; qPCR, quantitative real-time polymerase chain reaction; SDS-PAGE, sodium dodecyl sulfate polyacrylamide gel electrophoresis; MMP, matrix metalloprotease.

FIGURE LEGENDS

FIGURE 1. Decorin inhibits VEGFA-mediated angiogenesis by attenuating proangiogenic factors. A, RT² PCR Profiler Angiogenesis Array evaluating proangiogenic gene expression changes in HeLa cells following exposure to 500 nM decorin after 24 h. B, PCR array target gene verification performed via quantitative Real Time PCR (qPCR) under the same conditions as in A. PCR Profiler Angiogenesis Array and all subsequent qPCR verification analyses were performed in triplicate among three independent experiments, normalized to the endogenous housekeeping gene, *ACTB*, and reported as average fold changes \pm SEM in agreement with the Comparative $\Delta\Delta$ Ct Method (please see Experimental Procedures section for a full and detailed description).

FIGURE 2. Decorin potently attenuates VEGFA signaling. A, slot blot analysis of tumor conditioned medium in the absence or presence of 500 nM decorin following a 24 h incubation to evaluate effects on secreted VEGFA in cervical adenocarcinoma (HeLa), triple negative breast carcinoma (MDA-231), and normal human umbilical vein endothelial cells (HUVEC). B, quantification of secreted VEGFA signal intensity for the above described cell lines, normalized to total cell number. C, immunoblot analysis of HeLa, MDA-231, and HUVEC cell lysates treated in the presence or absence of decorin (500 nM) for 24 h. Lysates were recovered and separated by 10% SDS-PAGE and probed for cellular VEGFA. β -actin served as an internal loading control. D, immunoblot quantification representing normalized fluorescence to β -actin for cellular VEGFA after decorin protein core treatment. E, slot blot analysis of HeLa tumor cell conditioned medium treated with decorin protein core (500 nM) for the indicated time points. F, quantification of secreted VEGFA time-course for the time intervals analyzed. Immunoassayed proteins via slot blot and western blot were detected with IR-Dye conjugated secondary antibodies amenable for visualization via the Odyssey Infrared Imaging System (LI-COR) with data representative of 2-3 independent experiments run in duplicate and reported as mean \pm SEM (** p < 0.01, *** p < 0.001)

FIGURE 3. Decorin suppresses HIF-1 α and VEGFA in constitutively-activated HIF-1 α MDA-231 cells under normoxic conditions and suppresses critical transcription factors needed for HIF1A and VEGFA expression.

A, B, immunoblot analysis of HIF-1 α expression in either wild-type or mutant cell lines as indicated. Cells were exposed for 4 h to increasing concentrations of decorin. The lower parts of the blots were stained with Coomassie to demonstrate equal loading. The migration of molecular mass protein standards is shown on the left. *C, D*, immunolocalization of HIF-1 α and VEGFA in either wild-type or mutant cell lines as indicated. The cells were treated for 4 h with decorin, fixed, permeabilized and reacted with antibodies specific for either HIF-1 α or VEGFA. Bar = 10 μ m. *E*, quantification of secreted VEGFA obtained by slot blot analysis of media conditioned for 4 h by either wild-type or mutant cells as designated. *F, G*, gene expression analysis of critical pathway genes found to be essential for driving the expression of *HIF1A* and *VEGFA* after 4 h (*F*) or 24 h (*G*) of decorin as indicated. Data are representative of at least two independent trials run in quadruplicate and were normalized to the endogenous house keeping gene *ACTB*. Data are reported as percentage change \pm SEM as calculated according to the Comparative $\Delta\Delta$ Ct Method (* p < 0.05, ** p < 0.01, *** p < 0.001).

FIGURE 4. Decorin mediated attenuation of HGF/ Met signaling evokes potent angiostasis.

A, immunoblot verification of Met protein depletion following transient transfection of cognate targeting siRNA (80 pM) (designated as siMet) in HeLa 48 h post transfection. *B*, immunoblot analysis following positive verification of Met knock-down HeLa lysates probed for cellular VEGFA under conditions of control, decorin (24 h, 500 nM), siMet (80 pM), or combined treatment and appear as a quantification of cellular VEGFA fluorescent intensity after normalizing to β -actin. *C*, expression data gained from qPCR analysis of pertinent genes in the presence of siMet (80 pM). Verification of siRNA functionality is delineated in this graph for Met. *D*, HeLa lysates were immunoblotted for β -catenin and β -actin (as a loading control) under the influence of decorin (500 nM) for 24 h. *E*, HeLa cDNA libraries evaluated for *CTNBN1* via qPCR under the same experimental conditions as in *D*. *F*, micrographs depicting high resolution digital images of mouse dorsal skin as it appears from the interior, 14 days after subcutaneous injection with either Matrigel (80 ml combined with $\sim 10^6$ MDA-231 GFP⁺ cells) and HGF (10 ng/ml) in the absence (*F*, left panel) or presence (*F*, right panel) of decorin proteoglycan (200 nM). Asterisk denotes Matrigel plug and tumor location. *G*, morphometric analysis of blood vessel density reported as vessel intersections per μ m². Density was calculated by determining the average number of times the newly formed angiogenic vessels intersected a grid, representing a standard area of 1mm², which were superimposed onto the images. The values represent the mean \pm SEM (n= 600). Bar = 4 mm. Immunoblot and Met knockdown experiments represent an average of at least 2 independent experiments performed in duplicate with quantification representing the average \pm SEM for cellular VEGFA. Gene expression data are a representative of 2-3 independent trials reported as fold change \pm SEM (* p < 0.05, ** p < 0.01, *** p < 0.001).

FIGURE 5. Decorin prevents the expression and activation of matrix metalloproteases necessary for tumor extravasation, metastasis, and VEGFA liberation.

A, HeLa cell conditioned medium treated with PBS or decorin (500 nM) for 24 h was evaluated for enzymatic activity of MMP2 and MMP9 via gelatin zymography. *B*, quantification of MMP9 and MMP2 enzymatic activity as determined in *A* as a function of relative MMP activity. *C*, HeLa interrogated 24 h post decorin (500 nM) addition for the expression of *MMP9* and *MMP2* transcripts via qPCR. *D*, ELISA of total MMP9 and MMP2 as indicated and found in HeLa cell conditioned medium (ng/ml/24h) in the presence or absence of decorin (500 nM). Gene expression changes are reported as the average fold change \pm SEM collated over 2-3 trials performed in quadruplicate and normalized to the housekeeping gene *ACTB*. Gel zymography and total MMP2/9 ELISA were repeated twice in triplicate (* p < 0.05, *** p < 0.001).

FIGURE 6. Decorin induces the anti-angiogenic factor, thrombospondin-1 both in cell cultures and in tumor xenografts.

A, B, media conditioned by HeLa exposed to either vehicle (control) or decorin (500 nM) for 24 h were evaluated for the presence of secreted thrombospondin-1 and perlecan (as control). Notice that the levels of thrombospondin-1 are significantly elevated by exogenous decorin (*** p < 0.001, n=4). The values were obtained by utilizing dot blots with serial dilutions of conditioned media (400-12.5 μ l) and anti-thrombospondin-1 or anti-perlecan antibodies and reported as the relative signal intensities of either secreted thrombospondin-1 or perlecan, respectively. *C*, Western blot of cellular thrombospondin-1 from HeLa cells treated with or without decorin as indicated. *D*, tumor volume of HeLa xenografts at day 23. Mice bearing HeLa xenografts were treated with

Decorin Antagonizes Angiogenesis

intraperitoneal injections of decorin (5 mg/Kg) every other day over a period of 23 days ($***p < 0.001$, $n=6$ per group). *E*, induction of thrombospondin-1 in the tumor xenografts by systemic delivery of decorin. The images show representative frozen sections of HeLa xenografts at day 23 post-decorin treatment or control immunostained for thrombospondin-1. All micrographs were imaged using the same exposure and gain. The right panels are 3D surface plots of the corresponding images to the left which were generated with ImageJ software as described before (47). Bar $\sim 10 \mu\text{m}$. *F,G*, qPCR analysis of mRNA extracted from HeLa xenografts at day 23 post-decorin or control treatment. Data are from three independent trials run in quadruplicate and normalized to the endogenous house-keeping gene *ACTB*. ($***p < 0.001$).

FIGURE 7. Schematic representation of proposed model for decorin-evoked angiostatic activity. Please refer to the text for a detailed explanation.

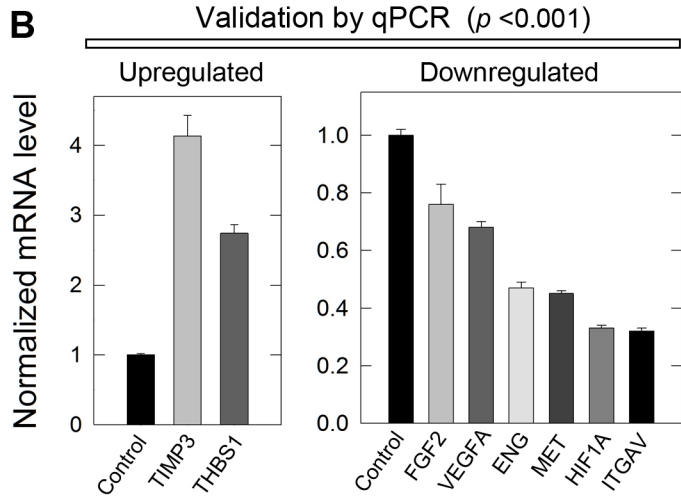
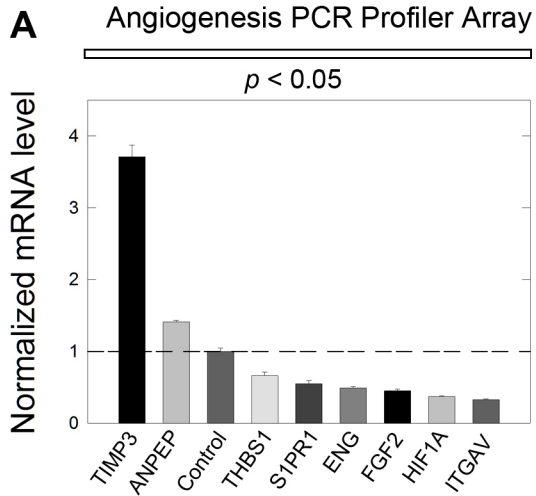


Figure 1

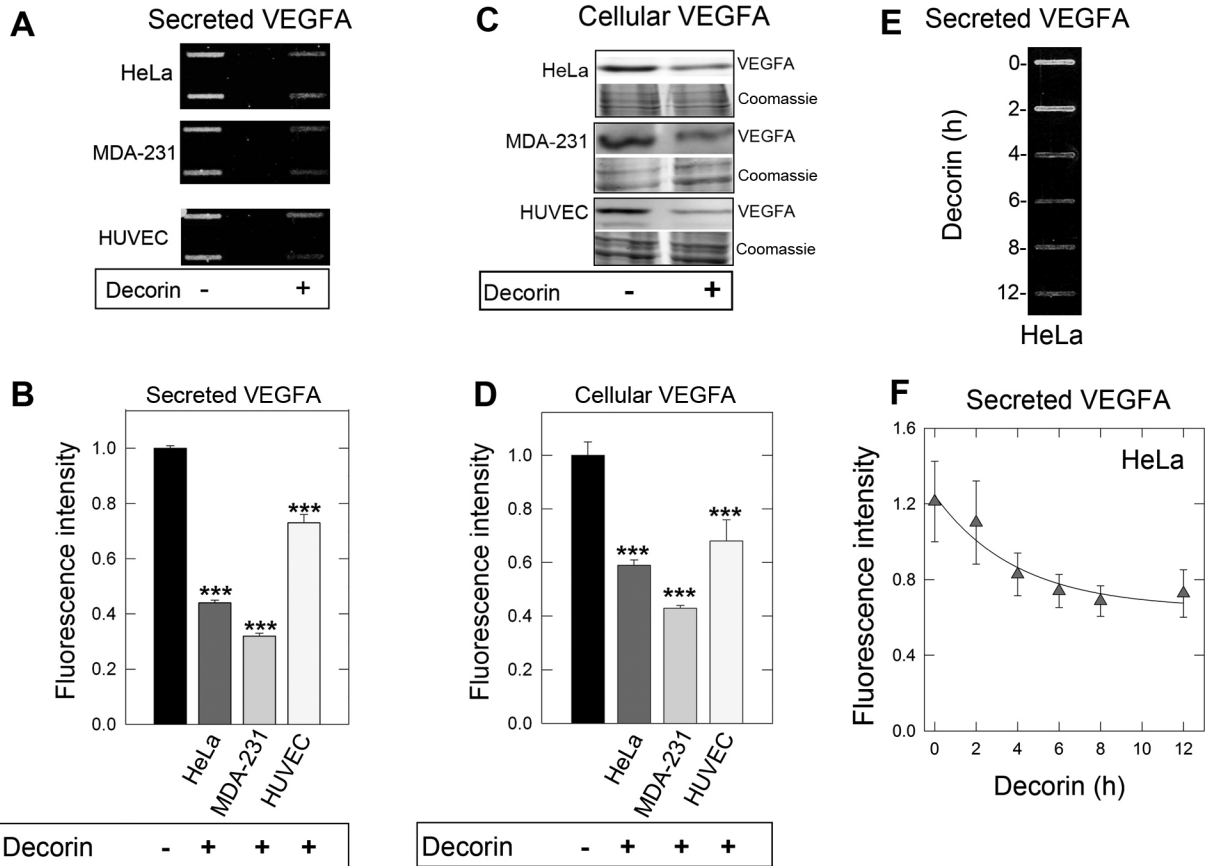


Figure 2

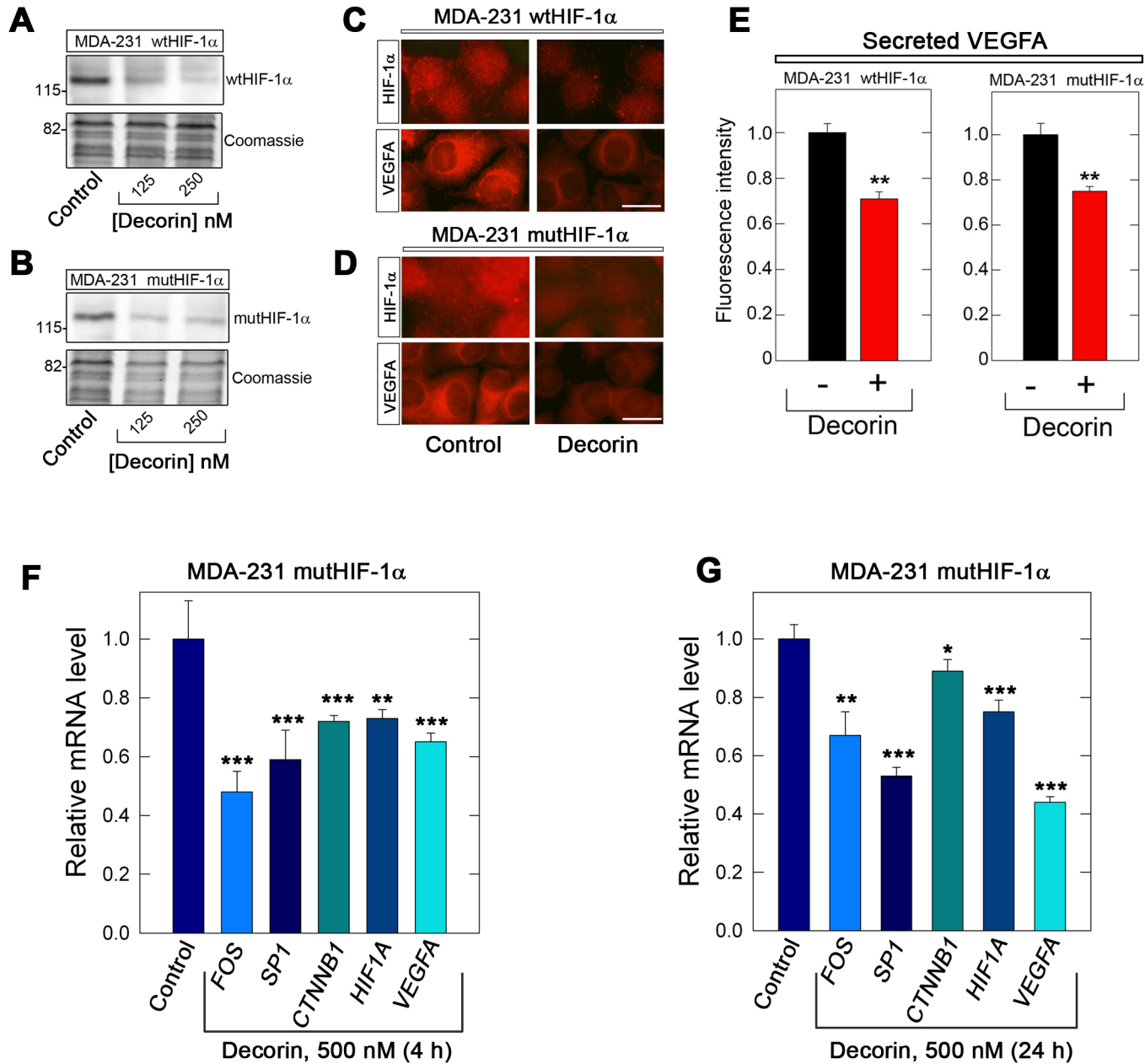


Figure 3

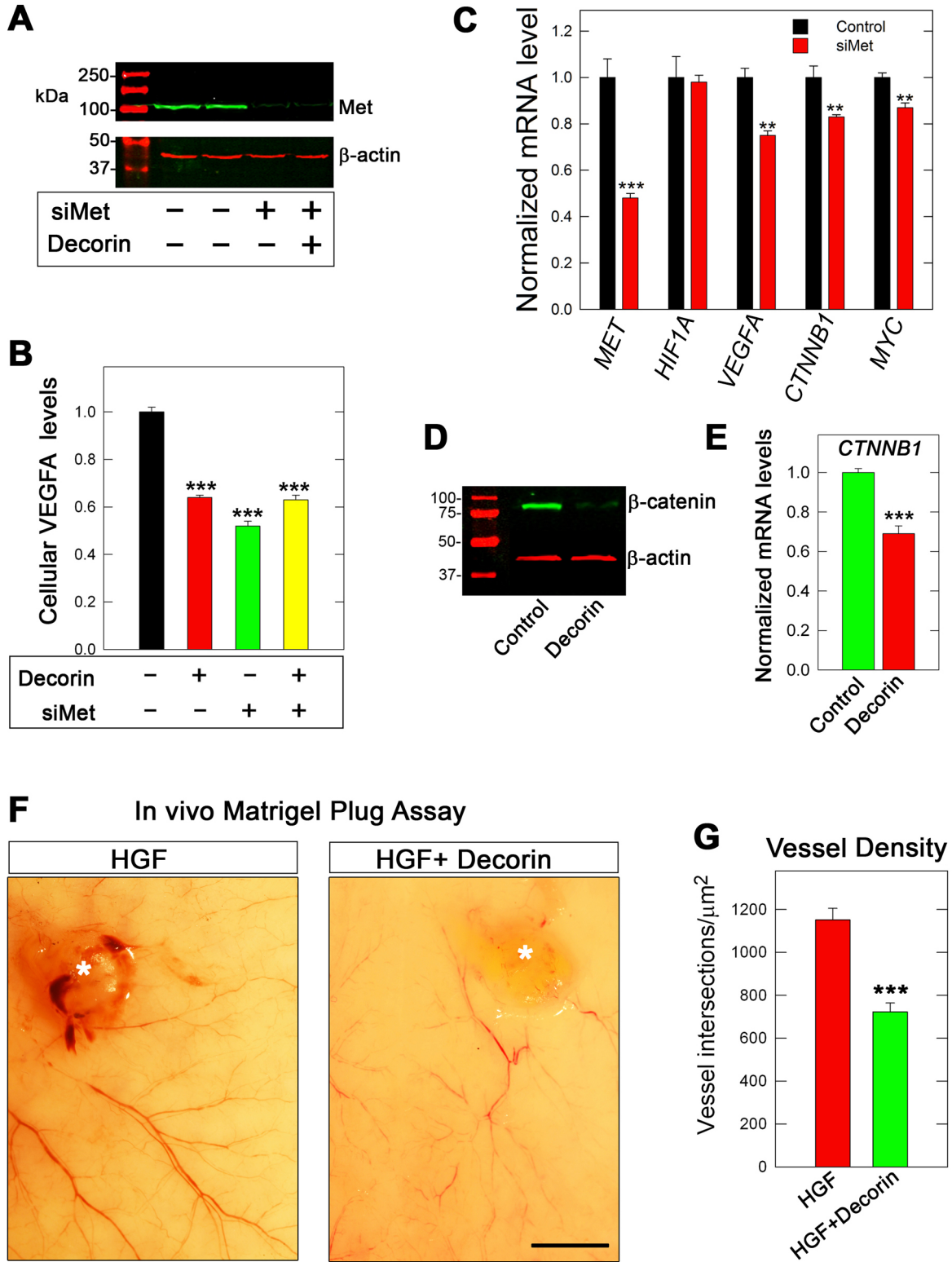


Figure 4

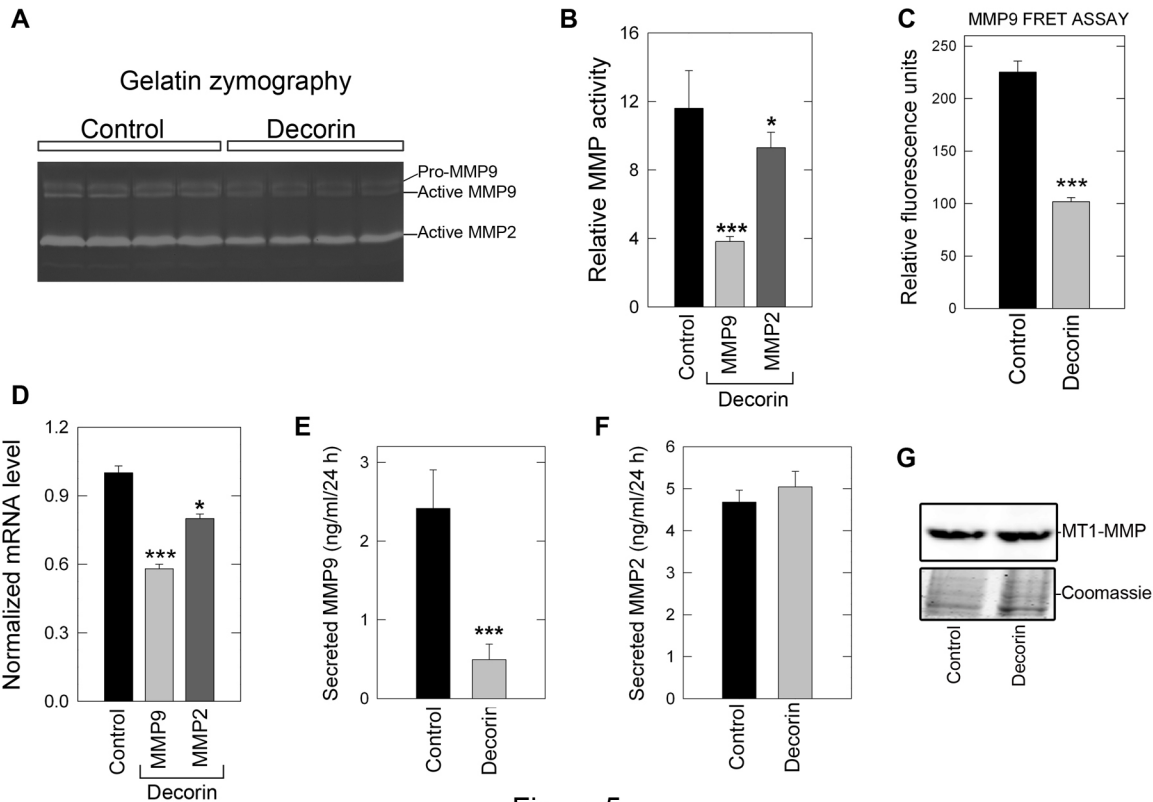


Figure 5

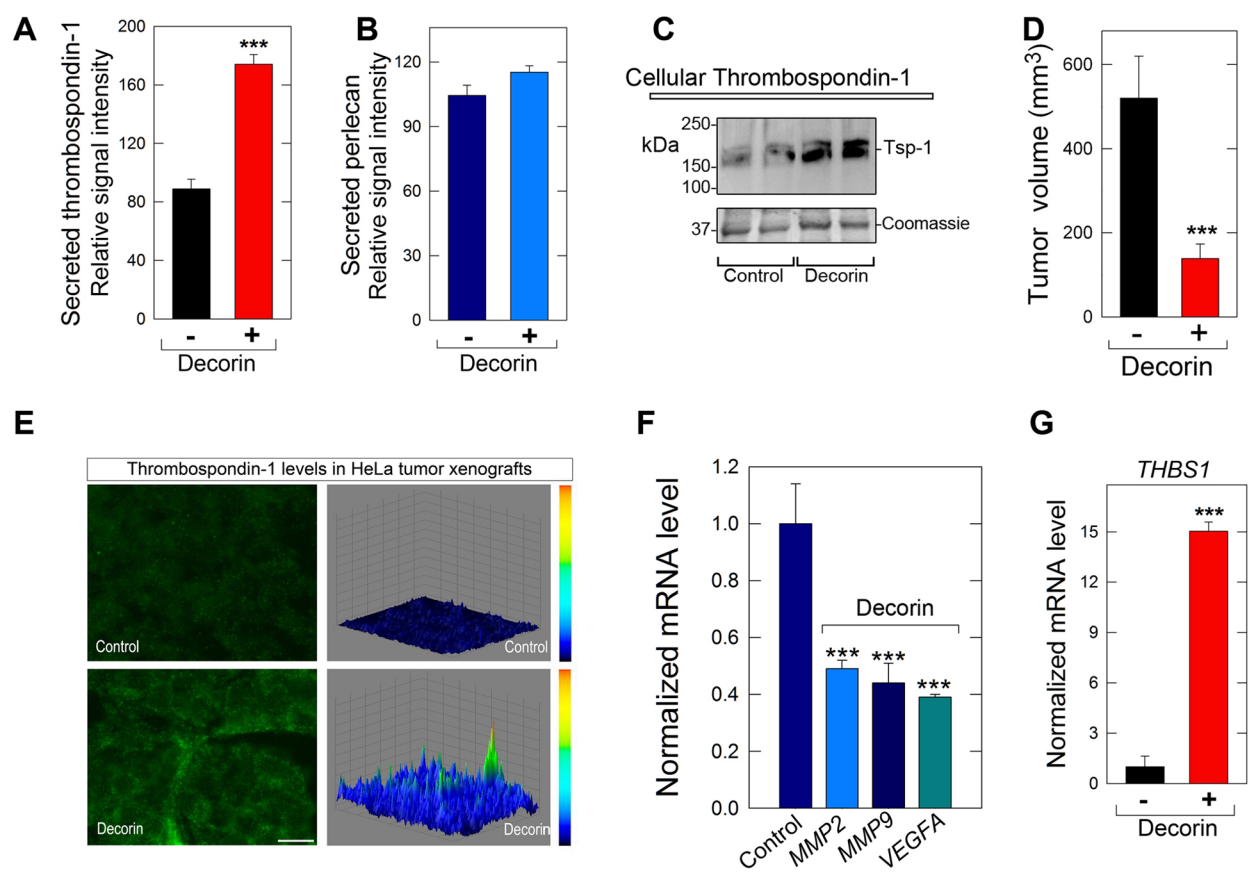


Figure 6

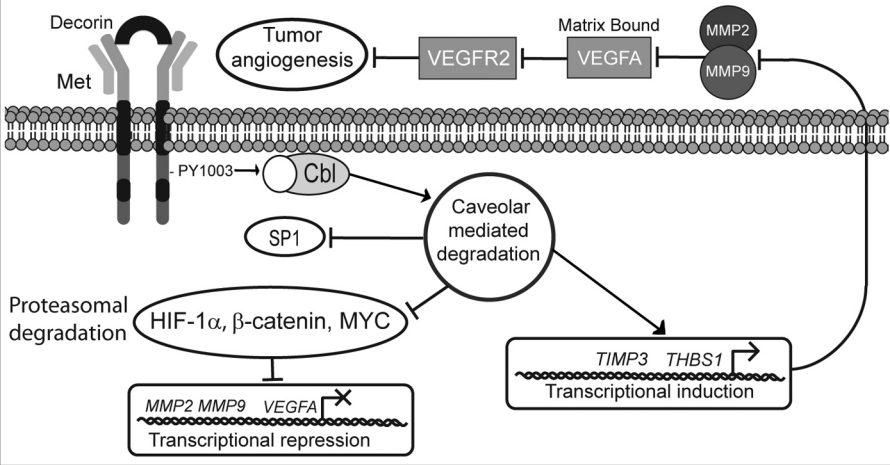


Figure 7